

## The Streaming Effect Coming from Gap Like Property in the Multi-group Diffusion Calculation

Eun Hyun Ryu <sup>a\*</sup>, Han Gyu Joo <sup>b</sup> and Jong Yub Jung <sup>a</sup>

<sup>a</sup>Korea Atomic Energy Research Institute, 1045 Daedeok-daero, Yuseong-gu, Daejeon, 34057, Korea

<sup>b</sup>Seoul National University, 599 Gwanak-ro, Gwanak-gu, Seoul, 08826, Korea

\*Corresponding author: ryueh@kaeri.re.kr

### 1. Introduction

Although we seldom conduct multi-group calculations at the lattice level, there are exceptions such as the pin-by-pin SP<sub>3</sub> calculation. In addition to the pin-by-pin style calculation, recently, PHWR channel calculation is being done to analyze the effects from pressure tube deformation. Because of the geometric limitation of the lattice calculation codes during this analysis, a finite element method (FEM)-based code, the Diffusion Equation Targeted and Finite Element-based Numerical Analyzer (DEFENS) code is used [1].

Because the DEFENS code is also a kind of multi-group diffusion solver as well, it should be provided with multi-group cross sections despite that its origin involves the homogenization using Monte Carlo Method-based code or pre produced properties. During analysis of PHWR, the McCARD code is used to provide homogenized region-wise 2 group cross sections with cut off energy of 0.625eV.

Using these cross sections, channel analysis in the PHWR was done and as a result, it was possible to observe quite strange distributions for fission source, and actual rapid thermal flux, during process of applying the superhomogenization (SPH) factor. Unlike the results of the McCARD code (a nearly flat distribution along with axial direction in the PHWR), it appeared the same as in the refueling direction.

During investigation on this phenomenon, inductive our inductive conclusion was that using the gap cross section which has large diffusion coefficient (extremely small total cross section, reversely) finally results in streaming effect.

In this paper, several problems with relatively simple geometric structure that depend on gap existence are examined by comparison between the Finite Difference Method (FDM)-based code, an in-house code, an FEM-based code, and the McCARD code.

### 2. Cross Section Generation

A lattice calculation was done for the fresh fuel-zero burnup-state. Owing to the sub-channel analysis characteristics, the coolant region was subdivided as shown in Fig. 1. Moreover, to incorporate the difference related to a distance from the center, the fuel region was divided into four regions which are called as the array. The remaining four cross sections (including for the pressure tube, gap, calandria tube, and moderator) were

generated by following a conventional method, specifically, the (n,2n) and (n,3n) types were grouped into a scattering cross section.

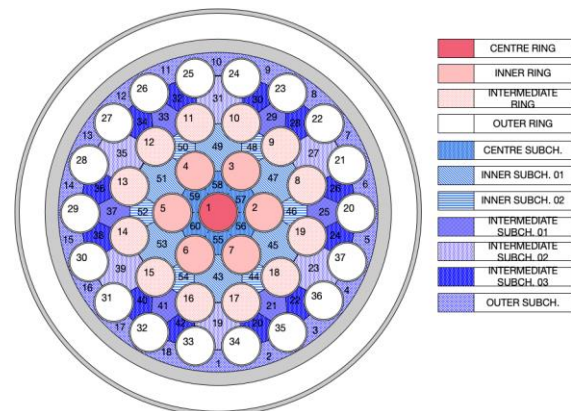


Fig. 1. Lattice Regions including Sub-channels

For the lattice McCARD calculation, 500,000 particle and 500 total cycles (including 100 inactive cycles) were used [2]. The gap between a fuel pellet and its cladding was filled with the same material with the same cladding material, while the gap between the pressure tube and calandria tube was depicted as it is. As can be seen in the Fig. 1, a very large amount of the overall area constitutes a CO<sub>2</sub>-filled gap. Ultimately, 15 cross sections were produced.

### 3. Problem Geometry and Streaming Effect

Due to the existence of a large gap between the pressure tube and calandria tube, substantial neutron leakage will occur at the axial boundaries. Thus, among the 14 layers (each one 50cm high), 12 layers have the same cross sections as in the lattice calculation. The first and last layer of moderator cross section produced in the lattice calculation, was used again to temporarily seal against the escape of neutron.

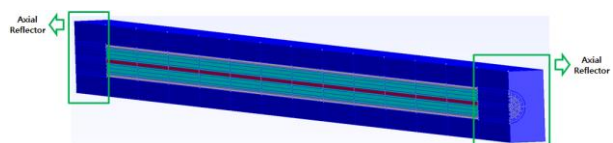


Fig. 2. Modeling of the Pressure Tube Analysis

The eigen values from the McCARD code calculations for infinite lattice, calculation with continuous cross section and axial reflector, calculation

with multi-group and axial reflector and the DEFENS code calculation with axial reflector are listed in Table I. The parts inside parentheses stand for the standard deviation of the McCARD code and error of the DEFENS code compared with the eigen values of the McCARD code calculation

Table I: Eigen Values of PHWR Channel Analysis

McCARD			DEFENS
Infinite Lattice (Case A)	Channel with REF. (C.X, Case B)	Channel with REF.(M.X, Case C))	Channel with REF.
1.12178 (5)	1.11353 (3)	1.10425 (3)	1.11300 (-878,-53,875)

In addition to this eigen values-related information, the power errors are also presented below (Table II).

Table II: Power Errors of the DEFENS code Compared with the McCARD code

Error Types	Case A	Case B	Case C
RMSE <sup>1)</sup> (%)	3.50	3.48	2.88
MAXE <sup>2)</sup> (%)	4.69	4.64	3.67
MAXE POS. <sub>3)</sub>	Pin 01	Pin 01	Pin 10

- 1) RMSE : Root Mean Square Error
- 2) MAXE : Maximum Error
- 3) MAXE POS. : Maximum Error Position

Taking a look at Table II, it seems that the RMSE is natural. Actually, the RMSE in this table comes from the axially integrated power. Thus, it does not guarantee that the axial distribution has a similar degree of error. The confirmation that the axial distribution does not match the reference McCARD calculation result occurs naturally from comparison of the eigen value. Even though the SPH factor was applied to the PHWR analysis, the eigen values did not match at all while the axially integrated power error matched it exactly. During the three-dimensional (3-D) power error calculation, it was found that the axial distribution did not match at all. Before being aware of the uniform distribution, various attempts were made to fit the eigen values. Among these attempts, was one to get the manual albedo iteration to fit the eigen value and the flux spectrum around the boundary/material interface.

The power and the fast and thermal flux distributions were plotted with albedo changes in relation to the McCARD calculation results for case A. It is noteworthy that every distribution shape is totally different from those of the McCARD code. Although all distributions types of the McCARD code were rather close to a cosine shape, all types of distribution for the DEFENS code were almost uniform along the axial direction, including a sudden drop in the axial reflector region. The following figures show axial distributions of the target parameters, which proved impossible to

understand. Thus, a simple one-pin problem was solved again to simplify the problem; the cross sections were utilized again for this simpler problem.

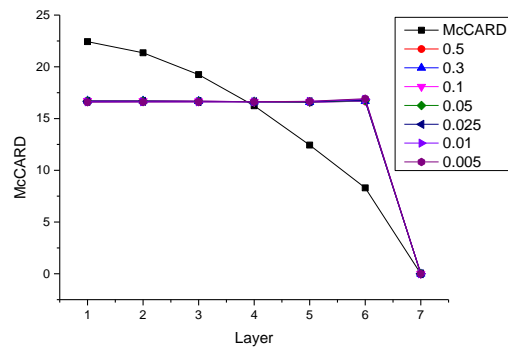


Fig. 3. Normalized Axial Power Distribution

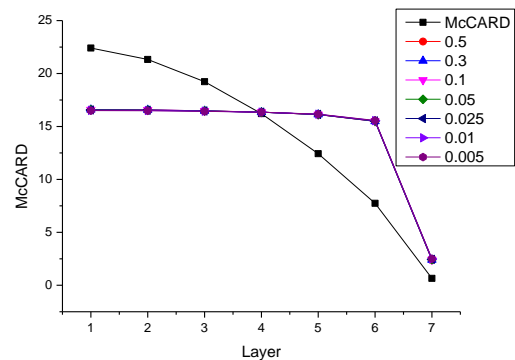


Fig. 4. Normalized Axial Fast Flux Distribution

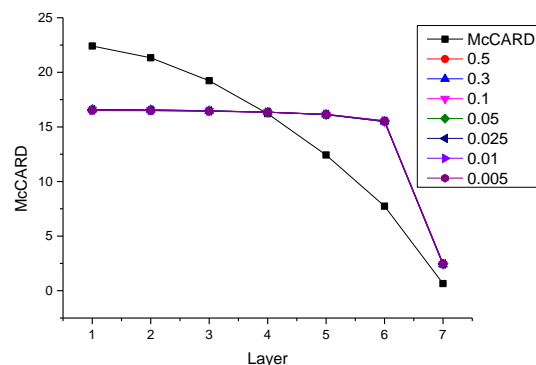


Fig. 5. Normalized Axial Thermal Flux Distribution

The geometry is really simple, only one pin exists and the annulus structure includes the coolant surrounding the pin, the pressure tube enveloping coolant and pin, the CO<sub>2</sub> gap outside of the pressure tube, the calandria tube containing the entire annulus region and finally, the square moderator similar to the pressure-tube-channel geometry. The dimensions for each region are given as radii of 1cm for fuel, 2 cm for coolant, 2.5 cm for the pressure tube, 3.0cm for a gap, 3.5cm for the calandria tube, and finally, a 20 cm square.

In Fig. 6, a cross sectional view can be confirmed. This geometry, with length of 350cm and 10cm height has 35 layers. To see the boundary condition dependency, two cases were examined that reflective B.C. (Case 1) and vacuum B.C. (Case 2). Following are the tables with eigen values and distribution of fission sources and of the fast and thermal flux. The numbers inside the parentheses in the McCARD and DEFENS columns mean the standard deviation and pcm error-unit compared with the McCARD code result. Note that the average pitch of the DEFENS code for this problem is 0.625cm.

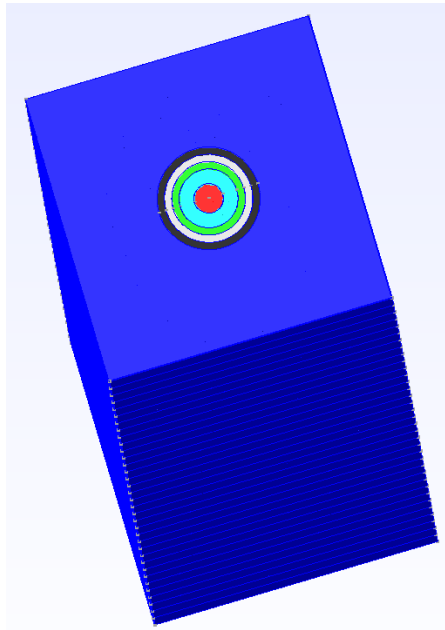


Fig. 6. Simplified One Pin Problem including Cylinder Geometry

Table III: Eigen Values for Simplified Cylindrical Problem with GAP Material

	McCARD	DEFENS
Case 1	0.84415 (3)	0.84629 (214)
Case 2	0.83567 (3)	0.81358 (-2209)

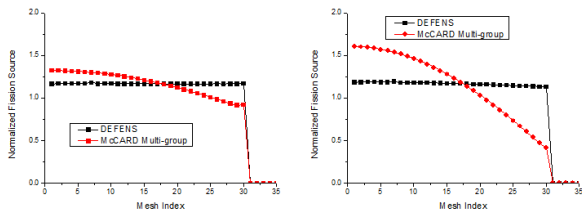


Fig. 7. Axial Fission Source Distribution for Case 1 and 2(with Gap, cylindrical problem)

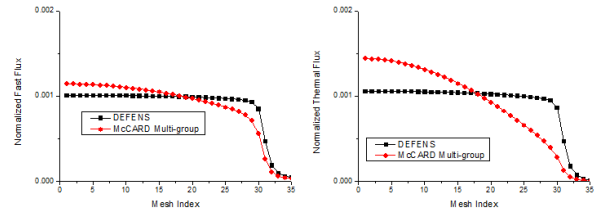


Fig. 8. Fast Flux Distribution for Case 1 and 2(with Gap, cylindrical problem)

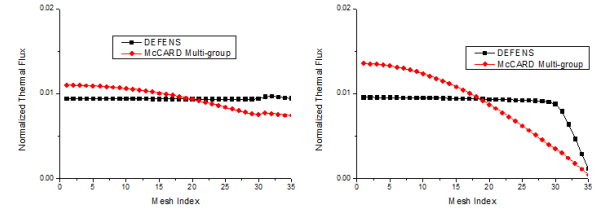


Fig. 9. Thermal Flux Distribution for Case 1 and 2(with Gap, cylindrical problem)

Although we simplified the geometry, the uniform distribution along the axial direction was retained as in the previous PHWR analysis. It was impossible to see any change in the z-direction; however, sometimes a tiny increase in value occurred along the axial direction. Thus, several tries were made to accommodate this phenomenon by such as gap filling, tightening convergence criteria, and so on. In the end, it turned out that only gap filling or removing gap material was effective. We determined that the neutrons were free to move through gaps to other regions, so no clear distribution was apparent. From here, the results presented are those found after replacing the gap material with calandria tube material.

Table IV: Eigen Values for Simplified Problem w/o GAP Material

	McCARD	DEFENS
Case 1	0.73912 (2)	0.73943 (31)
Case 2	0.73296 (2)	0.73286 (10)

After filling the gap region with calandria tube material, the similarity between results from DEFENS and McCARD increased incredibly, becoming almost the same. Although several other problems (aside from this problem regarding the existence of gap are not presented here, they support this conclusion sufficiently. Actually, the gap property itself is not a problem, but if whatever material chosen, has a large diffusion coefficient, reversely, an extremely low total cross section is a problem, that will make trouble. In Fig. 10-12, every result from DEFENS is surprisingly similar to those from McCARD. Namely, after removing the gap material streaming effect in the channel disappeared. Moreover, a cosine shape for vacuum B.C. (Case 2) can be observed. If someone looked up the thermal flux

distribution in more detail, he or she would find that a peak would appear near the material boundary. Of course, the fast flux would rapidly vanish from the boundary region between the fuel and axial reflector, because most of the fast neutrons would be moderated in an instant. Thus, the population involved in the fast flux between two material interfaces would drop in a second.

In Table V, the multi-group properties of the gap material are listed. It is noteworthy that large diffusion coefficients for both groups (between 1000 and 2000) with cut off of 0.625eV can be observed. This is difficult to observe in other material properties.

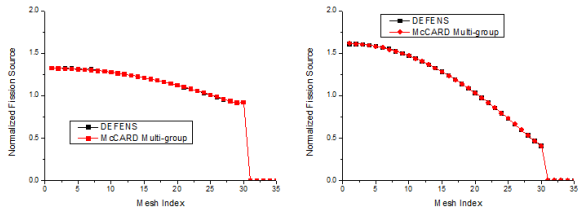


Fig. 10. Axial Fission Source Distribution for Case 1 and 2(w/o Gap, cylindrical problem)

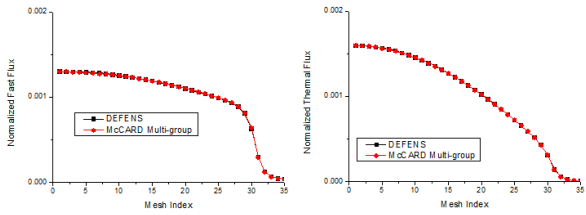


Fig. 11. Fast Flux Distribution for Case 1 and 2(w/o Gap, cylindrical problem)

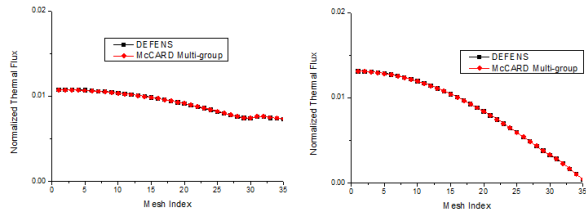


Fig. 12. Thermal Flux Distribution for Case 1 and 2(w/o Gap, cylindrical problem)

Table V: 2 Group Properties of the GAP Material

	Group 1 (Fast)	Group 2 (Thermal)
Diffusion ( $D_1, D_2$ )	1.828181E+03	1.588873E+03
Removal ( $\Sigma_{r1}, \Sigma_{r2}$ )	1.349646E-06	1.533279E-07
Nu-fission ( $\nu\Sigma_{f1}, \nu\Sigma_{f2}$ )	0.000000E+00	0.000000E+00
Chi-spectrum	1.000000E+00	0.000000E+00

$(\chi_1, \chi_2)$		
Scattering to Other ( $\Sigma_{s,down(1 \rightarrow 2)}, \Sigma_{s,up(2 \rightarrow 1)}$ )	1.298550E-06	1.094440E-07

Because many verifications of the DEFENS code have already been done, it is certain that there are not major problems in the code itself. However, to make sure, a Finite Difference Method (FDM) based code was used to explore the same streaming effect problem involving the gap material. To make the problem simple and utilize the FDM code, the geometry was made simple as possible. The following rectangular geometry was used to run the FDM code (Fig. 13). Two cases (reflective and vacuum B.C.) were considered as in the previous simple cylindrical problem.

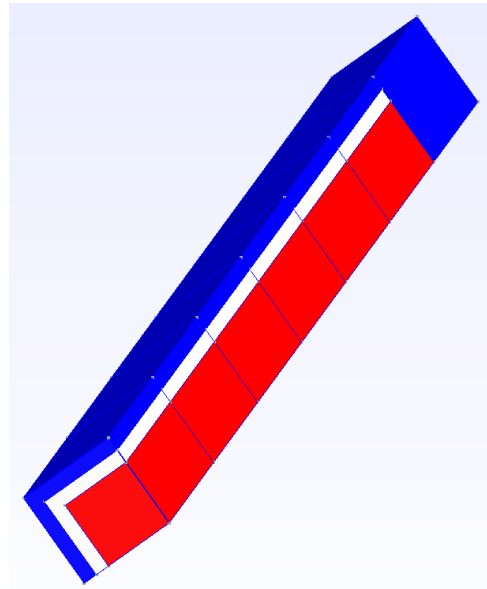


Fig. 13. Simplified Problem including Rectangular Geometry and Gap Material

Table VI: Eigen Values for Simplified Rectangular Problem with GAP Material

	McCARD	DEFENS (FEM)	FDM
Case 1	0.87390 (11)	0.85222 (-2168)	0.85072 (-2318)
Case 2	0.84152 (5)	0.84397 (245)	0.84533 (381)

As can be seen in Table VI, the difference between DEFENS and the FDM code is very small in spite of the difference in the pitch size (0.585cm and 1.414cm for DEFENS and the FDM code, respectively). However, if we take into account the gap material, the difference between the transport code and the diffusion code increases substantially. Considering this fact, when we solve a problem including material with a large

diffusion coefficient, it can be assumed that the difference between the transport code and the diffusion code goes up. The same trend can be observed for the fission source, fast flux and thermal flux results. This is because the in-house FDM-based code has also been verified many times, and this code also has no problems.

[1] E. H. Ryu and H. G. Joo, Finite Element Method Solution of the Simplified P<sub>3</sub> Equations for General Geometry Applications, Vol.56, p. 194-207, 2013.  
 [2] H. J. Shim and C. H. Kim, McCARD User's Manual Version 1.0

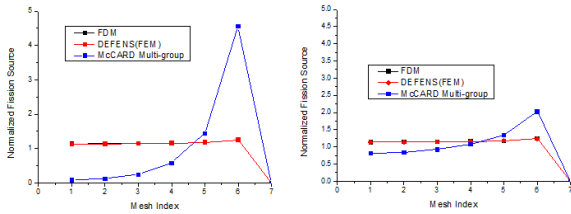


Fig. 14. Axial Fission Source Distribution for Case 1 and 2(w/o Gap, rectangular problem)

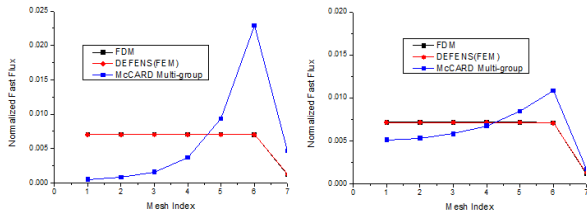


Fig. 15. Fast Flux Distribution for Case 1 and 2(w/o Gap, rectangular problem)

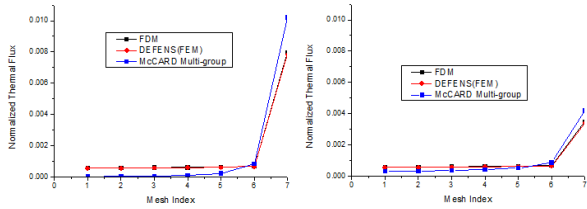


Fig. 16. Thermal Flux Distribution for Case 1 and 2(w/o Gap, rectangular problem)

#### 4. Conclusions

In this study, the ‘streaming effect’ is recognized and analyzed. For diffusion theory code, it is difficult to describe real phenomena in case that include materials with large diffusion coefficients. Although a solution is not proposed in this study, by reporting this phenomenon, additional analyses will become possible and continue into the future.

#### Acknowledgement

This work was supported by the National Research Foundation of Korea (NRF) grant funded by the Korea Government (Ministry of Science and ICT) (No. NRF-2017M2A8A4017282)

#### REFERENCES